Classical Dynamics of Harmonically Trapped Interacting Particles

Zhiyu Dong,[1,2] R. Moessner,[2] and Masudul Haque[2,3]

[1] *Department of Physics and State Key Laboratory of Surface Physics, Fudan University, Shanghai 200433, China*
[2] *Max Planck Institute for the Physics of Complex Systems, Nöthnitzer Str. 38, 01187 Dresden, Germany*
[3] *Department of Theoretical Physics, Maynooth University, Co. Kildare, Ireland*

(Dated: December 15, 2017)

Motivated by the interest in the dynamics of trapped quantum gases, we study the microcanonical dynamics of a trapped gas of classical particles interacting with a finite-range interaction of tunable strength. We examine two questions which have been of interest in quantum dynamics: (1) the breathing mode (size oscillation) dynamics of the trapped gas and the dependence of the breathing frequency on the interaction strength, and (2) the long-time relaxation and possible thermalization of the finite isolated gas.

I. INTRODUCTION

The non-equilibrium dynamics of isolated systems has been the subject of a large volume of work in recent years. In particular, in the quantum context, the study of unitary quantum evolution of many-body and few-body systems has undergone an explosive growth. This interest was partly fueled by the availability of experimental systems, e.g., trapped ultracold atomic and ionic systems, where non-dissipative dynamics can be studied explicitly due to excellent isolation. There are also foundational reasons for studying quantum dynamics in isolation: recent activity has led to advances in the understanding of basic principles connecting quantum dynamics, quantum chaos and the emergence of statistical mechanics and thermalization (CITE). For classical many-body systems, explorations of the connections between microscopic dynamical rules, chaos, ergodicity and statistical mechanics have a much longer history, dating back to the time of Boltzmann and Poincare [1–4].

Motivated by questions and issues arising in the field of quantum many-body and few-body dynamics, in this work we will study the classical dynamics of a collection of interacting particles confined in a one-dimensional harmonic trap. The analogs of two questions, studied intensively in the quantum literature, will be investigated for this classical system: (1) the influence of interactions on the breathing mode frequency of the trapped gas, and (2) the relaxation and possible thermalization of the finite system under its own evolution, in the absence of any external baths or dissipation mechanisms.

Experiments with cold atoms, which have an essential motivational role for the current interest in many-body quantum dynamics, are generally performed in a trapping potential, either optical or magnetic. As a result, in the last two decades many questions of many-body quantum physics have been reformulated in the presence of a harmonic trap. The presence of a harmonic trap often results in new dynamical phenomena. For example, the motion of vortices in a trapped condensate (CITE) has new features, such as precession, compared to vortex motion in uniform condensates (CITE). Trapping also results in new collective phenomena which have no analog in uniform situations: for example, collective modes like dipole, breathing and quadrupole modes are specific to trapped many-body systems. Dipole modes (center of mass oscillations) and breathing modes (size oscillations) appear even for one-dimensional trapped systems; higher-dimensional systems display additional, more complicated modes like quadrupole and scissors modes. Because of the omnipresence of trapping potentials in cold-atom experiments, dipole and breathing mode dynamics are pervasive across the field: These modes have been intensively studied and used for diagnostic purposes since the early days of research with trapped quantum-degenerate gases, and continue to generate interest today [5, 6, 8–14, 16, 17, 19? –25]. (CITE). In one of the best-known experiments on quantum many-body dynamics, Ref. [26], the dynamics of an integrable system (Lieb-Liniger bosons) was seen to have ultraslow relaxation in a trap, supposedly due to integrability. This experiment has led to continuing efforts to understand how a trap breaks integrability (CITE).

The presence of harmonic trapping is thus a paradigmatic aspect in the field of quantum non-equilibrium physics. This motivates our study of classical dynamics of trapped interacting particles. Similarly motivated by quantum dynamics, classical trapped dynamics of hard rods has recently been studied in Refs. [27, 28], focusing on integrability-breaking effects of the trap. In this work, we consider trapped classical particles which interact via a simple finite-range potential between any pair of particles: a constant repulsive force acts whenever the particles are less than a certain distance apart. The interaction strength can be tuned, leading to different regimes of behavior.

Our first theme will be the breathing mode of the classical interacting gas, and the effect of interactions on the frequency of the breathing mode. In the quantum case, this has long been a topic of interest for both bosons and fermions. For bosons with short-range (contact) interactions, the situation has been studied in one, two and three dimensions. At zero interactions, the breathing mode is twice the trapping frequency ω_0 in each case, assuming isotropic trapping. A mean field (Gross-Pitaevskii) calculation gives the frequency to be $\sqrt{D+2}$ times the trapping frequency, where D is the spatial dimension. For three-dimensional (3D) traps, the mean-field description can be expected to be qualitatively correct, thus the breathing mode frequency is expected to change monotonically from $2\omega_0$ at zero interactions to $\sqrt{5}\omega_0$ at large interactions. For 2D traps, the breathing frequency is exactly $2\omega_0$ for any interaction strength [7], due to a symmetry. Classical trapped particles with scale-invariant interaction potentials also have breathing frequency $2\omega_0$ independent of interaction strength [7]. The interaction dependence in 1D (trapped Lieb-Liniger gas) is also remarkable: as the interaction is increased, the breathing frequency first decreases from $2\omega_0$ to the mean-field prediction $\sqrt{3}\omega_0$, and then at larger interactions increases again, returning to $2\omega_0$ in the infinite interaction (Tonks-Girardeau) limit [5, 10, 11, 16, 22]. The breathing mode has also been investigated extensively for fermionic systems with contact interactions [13–15], and also for fermionic and bosonic systems with long-range interactions [23, 24]. The breathing mode has also been studied for a high-temperature trapped gas where a Boltzmann-equation description is valid, both theoretically [29] and experimentally [30].

In this work, we use an explicit microscopic model treated microcanonically, rather than a Boltzmann equation approach. Unlike the quantum case, the harmonic potential does not impose a length scale or an energy scale. The interaction range can thus be scaled away by a redefinition of length, i.e., by measuring lengths in units of

the interaction range. There are thus only two important parameters determining the system behavior, namely the interaction strength and the energy per particle. We find that the breathing mode frequency has a non-monotonic dependence on the interaction parameter. At small interactions, when the particles pass through each other, the effect of collisions is to slow down the dynamics, so that the breathing frequency drops below the non-interacting value $2\omega_0$. At very large interactions, the particles bounce off each other, a process which speeds up the size oscillations, resulting in the breathing frequency being larger than $2\omega_0$.

Our second theme is the process of relaxation at longer timescales, and possible thermalization. This topic is also motivated by intense recent research in the quantum context. In quantum isolated systems, thermalization is now understood in terms of the so-called eigenstate thermalization hypothesis (ETH), which postulates that in ergodic systems the expectation values of observables in individual eigenstates depend ony on the eigenenergy, and hence represents the thermal value (CITE). The connection to statistical mechanics is particularly difficult for explicitly finite systems, in which case ETH is to be understood in terms of finite size scaling (CITE). In classical systems, the connection between microscopic dynamics and statistical mechanics has been continually studied since the 19th century [1–4]. It is generally understood that systems with nonzero Lyapunov exponents, i.e., chaotic or ergodic systems, thermalize in the long-time limit, provided there are enough degrees of freedom. As in the quantum case, finite systems are particularly intricate. In finite systems, defining thermalization is trickier as most observables will fluctuate or oscillate substantially. In addition, the influence of Kolmogorov-Arnold-Moser (KAM) orbits may play a role in preventing thermalization; it is generally believed that the fraction of phase space where KAM physics might be relevant decreases rapidly with particle number [2].

In our work, we examine the relaxation of our trapped interacting classical system, explicity for finite numbers of particles. We look for thermalization within finite timescales, by sampling single-particle energies periodically until such timescales and comparing the distribution of single-particle energies with the Boltzmann distribution. We show that whether or not the system thermalizes in this sense depends on the ratio of interaction strength and energy per particle. We also show that this result is reflected in the finite-time Lyapunov exponents of the system. We also examine another notion of thermalization, according to which a system is thermalized when it loses memory of initial state, by following the dynamics of the particle distribution in phase space. Remarkably, we find that one can observe energy thermaliztion even at timescales when the shape of the phase space distribution continues to perform seemingly coherent oscillations.

There is a significant literature on calculating Lyapunov exponents in model statistical-mechanics systems and thus exploring ergodicity [1] (CITE). This provides intuition of what types of microscopic interactions are likely to produce thermalizability, and is an important step in the program of understanding statistical mechanics "from the bottom up". However, we are not aware of a significant literature on following explicitly the microcanonical dynamics of statistical-mechanical or few-body systems. Several such studies have appeared recently (CITE), motivated by the quantum dynamics literature, like the present work. A few earlier studies have also examined thermalization dynamics in one dimensional gravitational systems [35, 36]. Investigating such real-time dynamics can be expected to provide insights on the timescales and microscopic mechanisms involved in the emergence of statistical mechanics from collections of particles.

This paper is organized as follows: In Section II, we introduce the Hamiltonian, identify and introduce the essential scales, and describe some aspects of the model and our simulations. The breathing frequency is treated in Section III. We explain the main features using both real-space and phase-space pictures of the interaction process, obtain estimates for the interaction- and energy-dependence of the frequency shift, and compare these predictions with numerics. Section IV treats relaxation and thermalization. We propose a condition for relaxation in reasonable timescales from considerations of few-body dynamics, compare the energy distribution with the Boltzmann distribution, show how the largest finite-time Lyapunov exponent distribution reflects the relaxation condition, and examine shape dynamics of the particle distribution in phase space. Concluding remarks appear in Section V.

II. THE MODEL AND ITS EQUILIBRIUM PROPERTIES

A. Model and Scaling

Our model for the interacting classical gas involves particles with a simple finite-range repulsive interaction. Two particles repel each other whenever they are within a distance σ from each other. The force of repulsion is a constant, F_0, within this distance and zero when the distance is larger.

$$\left| F(x) \right| = \begin{cases} F_0 & |x| < \sigma \\ 0 & |x| > \sigma \end{cases} \tag{1}$$

where $|x|$ is the distance between two particles. This equation describes the magnitude of the interparticle force; the direction is always repulsive.

The gas contains N such identical particles, each of mass m, in a harmonic trap. The Hamiltonian describing the gas is

$$H = \frac{1}{2} m \omega_0^2 \sum_i x_i^2 + \frac{1}{2} m \sum_i v_i^2 + \sum_{|x_i - x_j| < \sigma} F_0 \left(\sigma - |x_i - x_j| \right) \tag{2}$$

It is useful to rescale the quantities. We will measure distance, time, energy and force in units of σ, $1/\omega_0$, $m\omega_0^2\sigma^2$ and $m\omega_0^2\sigma$ respectively:

$$\tilde{x}_i = \frac{x_i}{\sigma} , \quad \tilde{H} = \frac{H}{m\omega_0^2\sigma^2} , \quad \tilde{t} = \omega_0 t , \quad \tilde{F}_0 = \frac{F_0}{m\omega_0^2\sigma} . \tag{3}$$

Eq. 2 is then rewritten as

$$\tilde{H} = \frac{1}{2} \sum_i \tilde{x}_i{}^2 + \frac{1}{2} \sum_i \left(\frac{d\tilde{x}_i}{d\tilde{t}} \right)^2 + \sum_{|\tilde{x}_i - \tilde{x}_j| < 1} \tilde{F}_0 \left(1 - |\tilde{x}_i - \tilde{x}_j| \right) \tag{4}$$

Through this rescaling, we have reduced the number of the parameters in our model to three: the energy $\tilde{H}$, the interaction strength $\tilde{F}_0$, and the number of particles N. The rescaling is equivalent to setting σ, ω_0 and m to 1; this is what we do in our numerical simulation. In the rest of this paper, we will use "E" and "F_0" to denote the reduced versions $\tilde{H}$ and $\tilde{F}_0$.

We will be concerned with the size of the cloud. We quantify the size through the root-mean-square of particle positions $\{x_i\}$,

$$R \equiv \left(\overline{x_i^2} \right)^{\frac{1}{2}} , \tag{5}$$

and refer to this quantity as the 'radius' or 'cloud radius'. In the dilute gas limit, there are few or no interactions occuring at most times. Thus the energy E is dominated by the trap energy, i.e., $E \approx m\omega_0^2 \sum_i x_i^2 = Nm\omega_0^2 R^2$, or, in our units,

$$E \approx NR^2 . \tag{6}$$

This approximation is good when the average distance betwen particles is much larger than the interaction range $\sigma = 1$, i.e., whenever $R \gg 1$, which is the regime we consider dynamics in. Another way of describing this dilute-gas regime is that the gas is far from the ground state (described in the next subsection). Neglecting the interaction energy to estimate E is reasonable even at very large interactions ($F_0 \gg E/N$), because for very large interactions, the particles behave as hard rods which bounce off each other very rapidly, so that at most instants one can expect no collisions to be taking place, provided the gas is dilute. It is also expected to be a good approximation at very small F_0 since we can then simply neglect the interaction energy. Thus, we will use this as a common estimate for R in terms of the energy.

B. Ground states

The lowest-energy state of the system has zero kinetic energy; in this state the particles find stationary positions which minimize the trap (potential) and interaction energies. The trap potential tries to squeeze the particles towards the trap center, while the interaction tries to push them apart.

Because of the 'Heaviside theta' form of our interaction, at large enough interactions (large F_0) the particles are spaced exactly at distance equal to the range σ, which is distance 1 in our rescaled units. The interaction is then effectively a 'hard-core' interaction.

At very small F_0, the particles in the ground state are close enough to the trap center that each particle interacts with every other particle. Equating the interaction force due to all the other particles with the trapping force, one finds that the position of the i-th particle is

$$x_i = \frac{2F_0}{m\omega_0^2} \left(i - \frac{N+1}{2} \right) = 2F_0 \left(i - \frac{N+1}{2} \right) \tag{7}$$
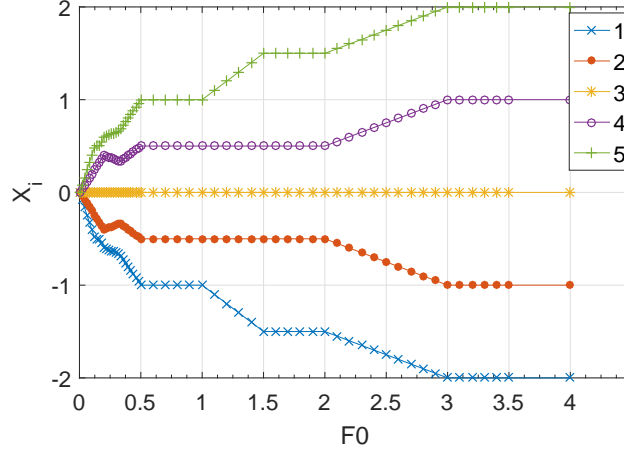
FIG. 1. The ground state of a system with $N = 5$ particles, shown via the positions of each particle, labeled 1 through 5. At large interactions, the particles position themselves just outside the range of interactions of the neighboring particles.

where the particles are labeled $i = 1$ to $i = N$ from left to right. Thus the particles are equidistant in this regime. In this 'solid'-like state, the low-lying excitation involves independent oscillation of the particles around their equilibrium position. In this regime, the distance between the leftmost and rightmost particles is at most $\sigma = 1$. Thus, this situation extends up to $F_0 = \frac{1}{2(N-1)}$. For the $N = 5$ case shown in Figure 1, this behavior is seen up to $F_0 < 1/8$.

In Figure 1, we can see this crossover from the "solid-like" limit (left) to the "hardcore gas" limit (right). In between, there is a rich staircase-like structure, as the particles attempt to minimize the interaction by being at distance > 1 from as many other particles as is compatible with the trap energy.

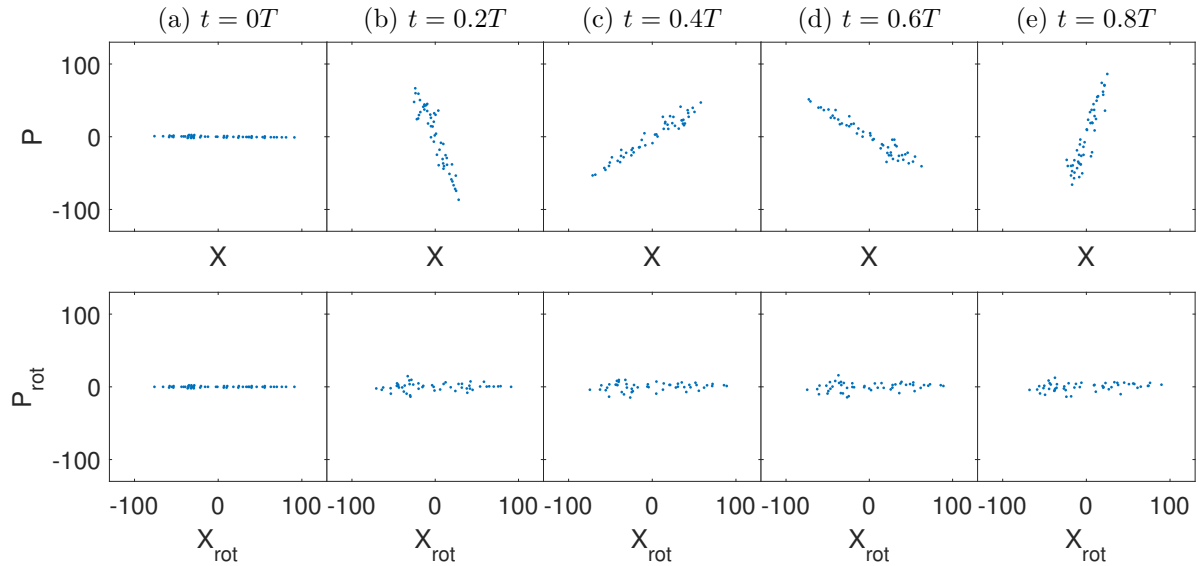## C.   Phase space distribution

FIG. 2. Upper (lower) panels are snapshots of the cloud configuration in phase space in the stationary (rotating) frame, at instants within the first trap period. Here $N = 50$, $F_0 = 100$, and $E = 50000$.

A useful way to visualize the state and evolution of the gas is to plot the position and momentum of each particle,
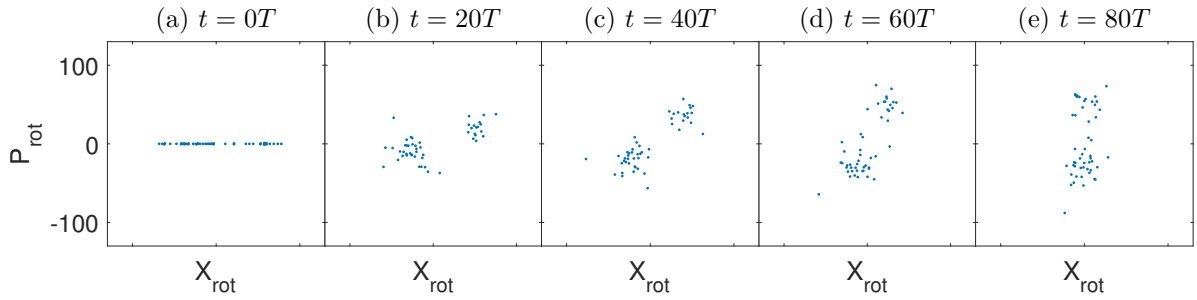
FIG. 3. Phase space snapshots of the cloud dynamics viewed in the rotating frame, at longer timescales. The broadening and rotation observed here are interaction effects: in the non-interacting gas the particles are stationary in this frame.

i.e., to plot the locations of the particles in the single-particle phase space. This will be useful for visualizing both the breathing mode and relaxation.

Figures 2 and 3 show such phase space snapshots. We generally start with particles distributed at random positions around the trap center, initially with no velocity (zero momentum). The initial state thus has the points lined up along the X axis. In the absence of interactions, each particle would undergo simple harmonic oscillation with period $T = 2\pi/\omega_0 = 2\pi$. The point corresponding to each particle executes clockwise elliptical motion around the X-P plane. (In our units, the elliptical trajectory is actually circular.) This results in the initial line remaining a straight line and rotating clockwise with exact period T. The effect of the interaction is to smear out the line and spread the points out toward a rotationally invariant distribution in the X-P plane. The top panel of Figure 2 shows this during the first period and Figure 3 shows this process over a much longer timescale.

Since the rotation of the initial line of points is simple to understand as a single-particle (non-interacting) effect, we can focus on interaction effects by viewing the phase space in a 'rotating' frame. The rotating frame is used in the lower panel of Figure 2 and in Figure 3. In this picture, the 'real' X and P axes are rotating counter-clockwise. This rotating frame picture may be regarded as a classical version of the "interaction picture" of quantum dynamics. This picture highlights effects of interactions because the other effects are already encoded in the frame rotation.

In the absence of interactions, each point (each particle) is stationary in the rotating-frame phase-space picture. As seen in lower panel of Figure 2 and in Figure 3, interactions cause a gradual distortion of the line as well as some degree of rotation. The rotation that is visible in the already rotating $X_{\rm rot}$-$P_{\rm rot}$ frame is the interaction-induced shift of the breathing frequency from the noninteracting value, $\omega_B = 2\omega_0$. The distortion of the line toward an eventually rotationally invariant distribution may be regarded as thermalization or ergodicity. In the next sections we explore these two interaction-induced effects.

D. Numerical calculations

We use the Verlet algorithm (molecular dynamics) to numerically simulate the cloud, using particle numbers between 5 and 50. Our force is simple, so that calculating the force at each step is inexpensive, however, the theta function dependence of the force on particle positions requires the use of fine timesteps at the beginning and end of each collision process.

The initial state is taken to have particles with zero velocity and random positions; hence the line distribution in the phase space picture. This has the advantage that the breathing motion is prominently visible. In addition, the question of long-time relaxation has the simple interpretation of evolving from the line distribution to a circularly symmetric distribution.

III. BREATHING FREQUENCY

We are interested in the oscillations of the size $R(t)$ of the cloud. It is convenient that our finite-size simulations start with a line distribution in phase space. If we started with a state whose configuration in phase-space deviates only slightly from circular symmetry, the oscillating amplitude would be too small to be distinguished from noise.

Without interaction, the breathing mode frequency is exactly 2. This is visualized readily from the top panel of 2, where $R(t)$ is the extent of the distribution in the horizontal (X) direction. As the line rotates clockwise with frequency $\omega_0 = 1$, within each period the line is twice horizontally aligned (maximum R) and twice vertically aligned
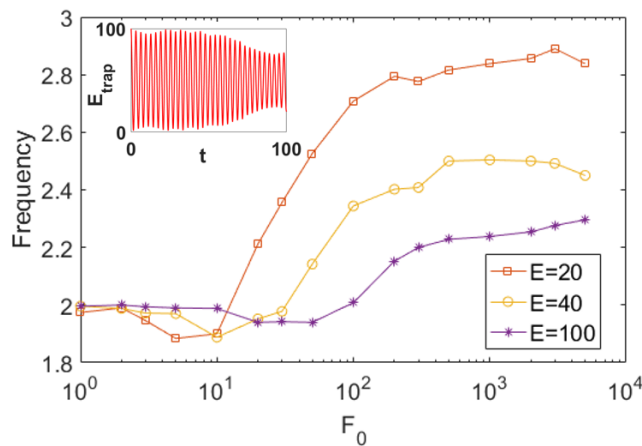
FIG. 4. Breathing mode frequency measured at different E and F_0, for $N = 5$ particles. Inset: a demonstration of the oscillation of E_{trap}, the total potential energy of particles in the trap, Since $E_{trap} \propto \sum_{is} x_i^2$, it manifests the oscillation behavior of the radius $R(t)$ as defined in Eq. 5. The breathing frequency is obtained from the Fourier transform of $R(t)$.

(minimum R), so that the frequency of $R(t)$ is $\omega_B = 2$. When there is interaction, the frequency will get shifted: $\omega_B = 2 + \delta$. Numerically, we measure the radius of the cloud $R(t)$ and get the frequency spectrum of its oscillation behavior by Fourier transform. Then we take the peak frequency near 2 as the breathing mode frequency.

A.   Interaction-dependence

The frequency measured numerically for different E and F_0 is shown in Figure 4 for a system with five particles, plotted as a function of F_0. The points each correspond to breathing-mode dynamics following from a single initial state; there is no averaging. The curves therefore show some noise. However, two prominent features are clear from these curves. At large interactions, $F_0 \gg E$, the breathing frequency is larger than 2, and saturates around a value which decreases with the system energy E. At small interactions, the breathing frequency is actually smaller than the non-interacting value 2.

Below, we will provide a detailed phase-space argument for these behaviors. However, a simple real-space picture explains both effects qualitatively as well. For very large F_0, when the interaction is 'hard-core'-like, two particles exchange momentum instantaneously during a collision. By exchanging the labels of the particles during the collision, this can be interpreted as follows: particle A carrying momentum P_A jumps by distance σ to the right, while particle B carries its momentum P_B and jumps by distance σ to the left. In this manner, every collision will save a particle some time, $\frac{\sigma}{v}$. This translates into an increase of the breathing frequency. The speed v per particle is on average $\sim \sqrt{E/N}$, and the number of collision each particle experiences in one period of harmonic oscillation is $\sim N$; hence we obtain $\delta \sim N^{\frac{3}{2}} E^{-\frac{1}{2}}$. When F_0 is smaller, we can no longer think of the particles as hard rods; the collisions now take finite time during which the speeds of the particles are actually slowed down and then sped up again, as they either cross paths or bounce from each other. When F_0 is small enough, this approaching time will at some critical value of F_0 consume the time saved by the finite range of the interaction. This explains why there is a small-F_0 regime for which the shift δ is negative. Figure 4 shows that this critical value of F_0, where δ changes sign and ω_B crosses 2, increases with energy.

B.   Estimates using the rotating phase space

Since we are interested in the deviation $\delta = \omega_B - 2$ from the non-interacting breathing frequency, it is useful to work in the rotating frame, in which a non-interacting cloud would be stationary (non-rotating). The rotation frequency of the cloud in this frame is then δ.

To analyze the rotation relative to the X_{rot}-P_{rot} frame, we consider two-particle collisions. In Figure 5(a), we show schematics of such a collision near the trap center at strong interactions. For very large F_0, the particles simply exchange momentum when they are at distance σ from each other; this process is shown in red as two straight lines. (The particles are initially at $X = \pm \frac{1}{2}\sigma$ and remain at these X values, but exchange their momenta.) For smaller
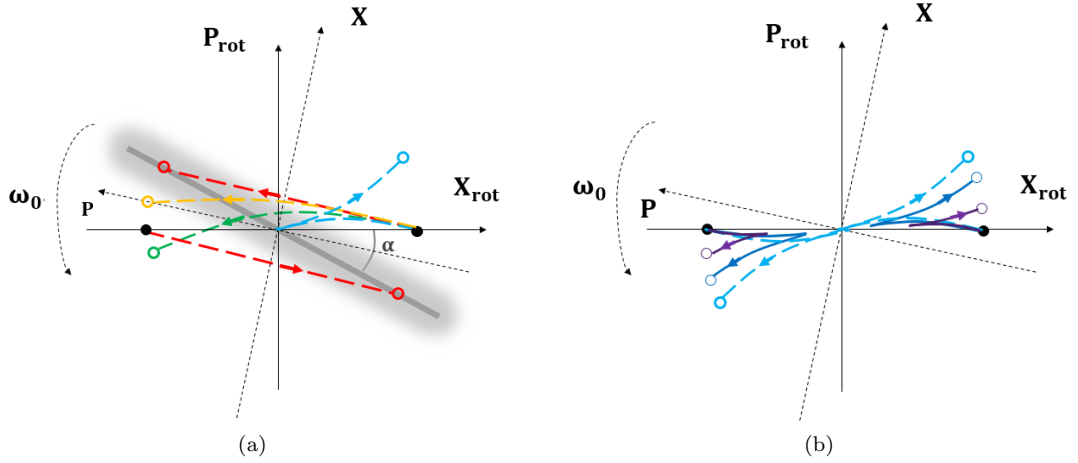
FIG. 5. Schematic diagrams of two-particle collision process in the $X_{\rm rot}$-$P_{\rm rot}$ plane. **(a)**When F_0 is large, particles cannot pass each other. Being subject to a constant repulsive force, their trajectories during collision are circular arcs. For very strong interactions (red dashed line, straight), they exchange momenta instantaneously. The yellow, green, and blue dashed curves are for successively weaker interactions. **(b)** When F_0 is small, particles pass each other, so that the force they feel is not continuous. Their trajectory has a turning point. The dashed bright blue trajectory is identical with the one in (a), which is the critical situation between passing and bouncing. In that case, particles have zero relative velocity when they collide.

F_0, there is change of both position and momentum, as shown in yellow, green and blue for successively weaker interactions. The blue line shows a case where F_0 is smaller enough such that the particles can actually cross each other.

In Figure 5(a) we show collisions for small F_0, so that the particles pass each other. The force changes direction discontinuously when the particles cross. In the $X_{\rm rot}$-$P_{\rm rot}$ plane, this is seen as a sharp turning point in the trajectory.

We now estimate δ at large F_0. The relevant collision process is that shown by the red lines in Figure 5(a). The two particles, which are initially on the $X_{\rm rot}$ axis, are moved to two other points, on the thick gray line, which deviates a small angle α away from original configuration. In every period of the harmonic oscillation, each particle meets each of the other particles twice. Half of these collisions (about N collisions) are between particles with large difference in momentum, which is the process shown in Fig.5. (As for the remaining half of the collisions, colliding particles have smaller difference in their momenta. In this estimate we ignore the effects of these collisions, as they clearly contribute far less to the rotation of the particle distribution.)

The precession angle is $\alpha \sim \sigma/P$. In our rescaled units, the typical momenta of interacting partilces is of the order R. (In phase space R can be interpreted either as the extent in real space when the velocities are small, or as the extent in momentum space when the particles approach $x = 0$, i.e. when the distribution is along the P direction.) Thus, we can estimate $\alpha \sim \sigma/R$, i.e., $\alpha \sim 1/R$, since our unit of length is σ. This is the rotation per unit collision. Since there are $\sim N$ collisions per period $T = 2\pi$, we have the estimate for the interaction-induced rotation per unit time as

$$\delta = 2\frac{N}{2\pi}\frac{1}{R} = \frac{1}{\pi}N^{3/2}E^{-1/2} \tag{8}$$

The factor 2 accounts for the fact that each rotation of the elongated cloud in phase space corresponds to two breathing mode periods. In the last step we have used the estimate $E \sim NR^2$.

The effect of interaction on breathing frequency is more complicated at smaller F_0. As we have seen in Figure 4, the effect of a small F_0 is to *decrease* the breathing frequency from its non-interacting value $\omega_B = 2$. This can also be understood using phase-space pictures of collision processes. For F_0 is not very big, the finite interaction time needs to be taken into consideration. During this time, the motion of each particle in phase-space is moving exactly along the direction of the real P axis at the rate F_0/m. Since the real P axis is rotating counter-clockwise, the particle will follow a circular trajectory, e.g., following the orange or green dashed lines in Fig. 5(a). The angle α that we used above to estimate δ thus decreases with the increase of interaction time; it is smaller for the yellow line and even opposite for the green line. This explains the negative contribution of interaction to δ, for small enough values of F_0. At even smaller values of F_0, shown in Fig. 5)(b), the particles cross each other. The resulting final values are such that the line joining the post-interaction locations of the two particles has negative α, i.e., is tilted clockwise with respect to the $X_{\rm rot}$ axis, meaning a negative contribution to the breathing frequency.

We can also estimate the critical value of F_0 for a given energy (or alternatively the critical value of E for a given F_0) between positive and negative contributions to the breathing frequency. Since the P axis rotates with frequency $\omega_0 = 1$ in the X_{rot}-P_{rot} plane, the post-collision position of the particle in the X_{rot}-P_{rot} plane makes angle $\omega_0 \tau$ with the red line in Figure 5(a). Here τ is the time over which the interaction acts. The crossover between positive and negative δ is found by comparing this angle to α:

$$\omega_0 \tau = \alpha \tag{9}$$

The time τ is approximately the time it takes for the momentum to change sign due to a constant force F_0, since the momentum is $\sim R$, this means $\tau \sim R/F_0$. Using our previous estimate $\alpha \sim \sigma/R$, together with $E \sim NR^2$, gives us the condition

$$\frac{E}{N} \sim F_0 \tag{10}$$

for the breathing frequency to cross the non-interacting value $\omega_B = 2$. This is roughly the same criterion for whether two particles will bounce or cross each other in a typical collision.

The condition (10) is consistent with Figure 4, where we noted that the critical F_0 grows with increasing energy.
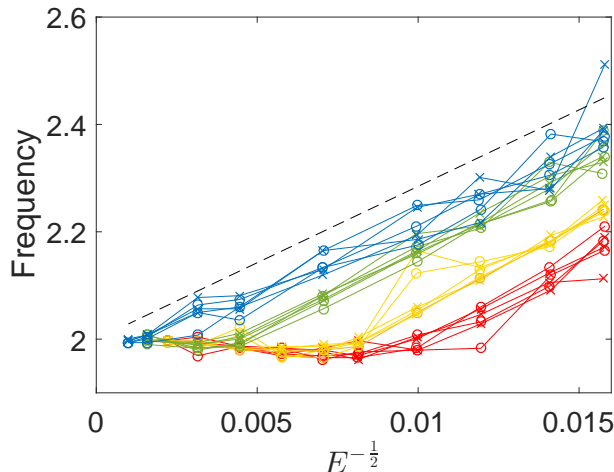
C. Comparisons with numerical data

FIG. 6. Dependence of breathing frequency, calculated for $N = 20$ particles, on energy. Different colors represent different F_0 — red for $F_0 = 2 \times 10^3$, yellow for $F_0 = 3 \times 10^3$, green for $F_0 = 1 \times 10^4$, and blue for $F_0 = 1 \times 10^5$. Runs with three different initial states are shown in each case. In each run, the frequency is measured both in the time window 0-100 (labeled as crosses) and in the time window 900-1000 (labeled as circles). The black dashed line is the prediction of Eq. (8).

In Figure 6 we show a quantitative test of the main rotating-phase-space prediction, Eq. (8). For large F_0, the frequency indeed scales as $E^{-1/2}$ and for $F_0 = 10^5$ is quite close to the actual numerical values prediction (8). Even for smaller F_0, at small enough energies (larger $E^{-1/2}$ values) the breathing mode becomes proportional to $E^{-1/2}$.

One might ask whether the breathing frequency predictions are also valid at late times, after the system has 'relaxed' from the initial line distribution in phase space to a more spread-out cloud, as we have seen in Figure 3. In Figure 6 we show the breathing frequency calculated from $R(t)$ oscillations in the first 100 time units, and also the frequency from data in a later time window. The frequencies appear to be overall stable and dependent primarily on F_0 and E.

IV. RELAXATION AND THERMALIZATION

For any nonzero interaction, the system is expected to be ergodic for $N > 2$. Once there are many particles, one expects thermalization in the long-time limit. From the few-particle perspective, several interesting questions pose themselves. First, although we expect ergodicity, the question of how long it takes to thermalize is an open question

for small N. We treat below a coarse-grained version of this question: namely, we ask whether particles show ergodic behavior within reasonable timescales chosen to be (somewhat arbitrarily) in the timestep range of 10^3–10^4. Another question is the connection between thermalization, as defined by the appearance of a Boltzmann distribution and other intuitive characteristics of ergodic behavior such as whether the single-particle phase space is isotropically occupied. We find cases where one aspect is seen while the other is not.

A. Few-particle considerations

Since we are interested in thermalization within finite timescales, it is useful to first consider mechanisms which hinder relaxation or thermalization. We begin with few-particle motion. Since ergodicity and relaxation are generally expected to be more robust and efficient with larger particle numbers, consideration of small particle numbers will highlight effects which slow down relaxation.
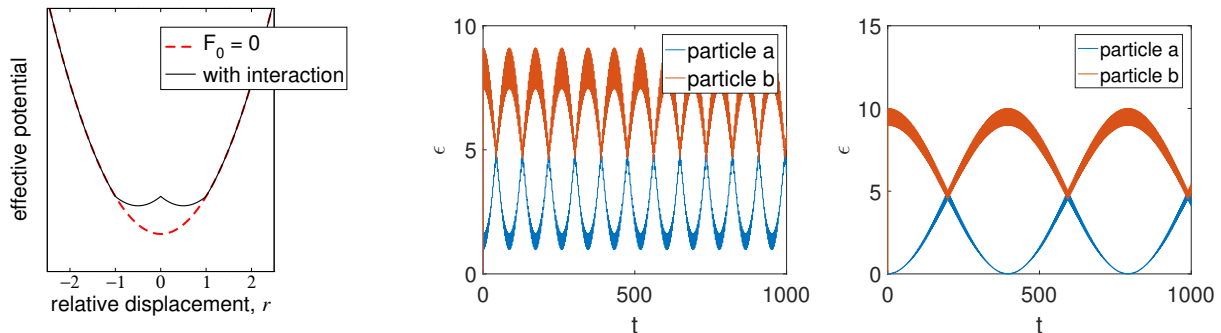

FIG. 7. Two-particle dynamics. Left: Effective potential for relative motion. Center and right: evolution of the individual energies of the two particles. The two panels correspond to internal energy $E_i = 2$ and $E_i = 5$; the interaction is $F_0 = 1$. The beat frequency is lower for larger E_i.

1. Two particles

We consider the two-particle motion in their center of mass frame. The center of mass itself executes simple harmonic oscillation. In the absence of interactions ($F_0 = 0$), the effective potential within the center of mass frame is itself parabolic, with the same frequency. So their relative motion is also a harmonic oscillation, with the same frequency ω_0.

With interactions, a term $F_0(1 - |r|)\theta(1 - |r|)$ is added, where r is the relative displacement; as shown in Figure 7. Now, the relative motion is no longer harmonic. When the internal energy is much larger than F_0, one could regard the resulting motion as having a slightly different frequency, or a collection of frequencies whose center is shifted slightly from ω_0. Since the center-of-mass motion is still of frequency ω_0, we have a superposition of slightly different frequencies, resulting in beating dynamics. This is clearly seen in the time evolution of individual energies shown in Figure 7. The two panels correspond to different internal energy E_i (defined as the total energy minus the center-of-mass energy). For larger E_i, the distortion of the effective potential (at constant F_0) plays a smaller role in shifting the effective frequency of relative motion; hence the beat frequency is smaller.

This illustrates a simple mechanism hindering the redistribution of energy between particles, which is necessary for thermalization or relaxation. As seen in the example dynamics shown in Figure 7, the difference in energy between the two particles is sustained over time. Of course thermalization is not expected anyway in a two-particle system, but we will see below how this basic effect continues to play a role for larger N.

2. More particles

Once we have more than two particles, we expect chaotic or ergodic behavior. However, it is easy to imagine mechanisms which drastically slow down redistribution of energy.

Generally, whenever we have some particles with energy very different from others, the dynamics occurs mostly independently within particle groups of different energies. For example, with three particles, consider the situation
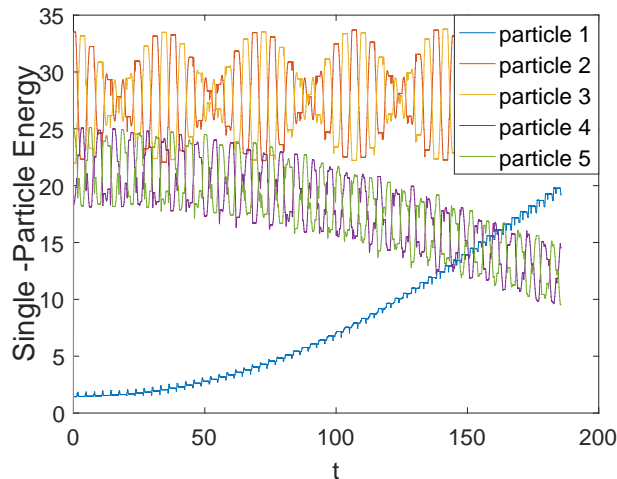
FIG. 8. Time evolution of single-particle energies in a system of five particles, showing a case of inefficient energy redistribution. The energies of the two particles with highest energy (4 & 5) show a clear beating similar to the two-particle case, as does the pair 2 & 3, although less visible. The 'unpaired' particle 1 performs slow beating dynamics with the center of mass of the 2 & 3 pair.

where two of them, say A and B, have small internal energy, which means their mutual distance and relative velocity are both small, whereas the third particle (C) has some energy quite different from A and B. Then, A and B will often be interacting, and if their internal is smaller than F_0, significant energy exchange can occur between them. C will generally exchange little energy with the pair during interactions, in which (due to larger internal energy between C and either A or B), the interaction is not effective in energy exchange. An example is shown in Figure 8, showing the dynamics of $N = 5$ particles. Two pairs of particles persist in performing 'internal' dynamics. The lone particle participates only in some slow beating motion with the center of mass of one of the pairs. Clearly, the energy mismatch acts as a hurdle to the relaxation process.

B. Relaxation condition and the Boltzmann distribution

Our consideration of few-particle motion has shown that relaxation is slow when the internal energy of pairs is large compared to F_0. This allows us to conjecture a condition for relaxation in reasonable time. Although it is impossible to express the internal energy of every pair in terms of the total energy E, we can estimate the typical internal energy by the average energy, $\frac{E}{N}$. At least they are of the same order. Thus we have the condition

$$F_0 \gtrsim \frac{E}{N} \tag{11}$$

for relaxation. This is the same condition we obtained for the breathing frequency to be increased (rather than decreased) by the interaction.

Because the model is expected to be ergodic for $N > 2$ particles, we expect the same condition to lead to thermalization. In fact, the proposed condition works even quantitatively, as we show in Figure 9. Here, the distribution of energies among the different particles is presented. Given our small particle number, a single snapshot of the energies will not yield enough statistics to investigate the distribution of single-particle energies. Therefore, single-particle energies are recorded once every time unit (i.e., at time intervals of $1/\omega_0$) as the simulation evolves, up to around $t \sim 10^4$. The distribution of these observed values then shows whether or not the system has thermalized to a Boltzmann distribution. In the two panels of Figure 9, we show the distributions obtained for a $N = 5$ system and a $N = 20$ system. In both cases, we choose the total energy to be $E = 1000N$. In accordance with our conjectured condition, we find that the observed single-particle distributions are qualitatively different for $F_0 \gtrsim 10^3$ and for smaller interactions. When the "thermalization condition" $F_0 \gtrsim E/N$ is satisfied, the distribution is roughly exponential ($\sim e^{-\beta\epsilon}$). For smaller F_0, thermalization in this sense is not seen in the single-particle energy distribution. Since the systems are expected to be ergodic, the smaller-F_0 systems presumably will also eventually show a Boltzmann distribution of energy, but only at (much) longer timescales.
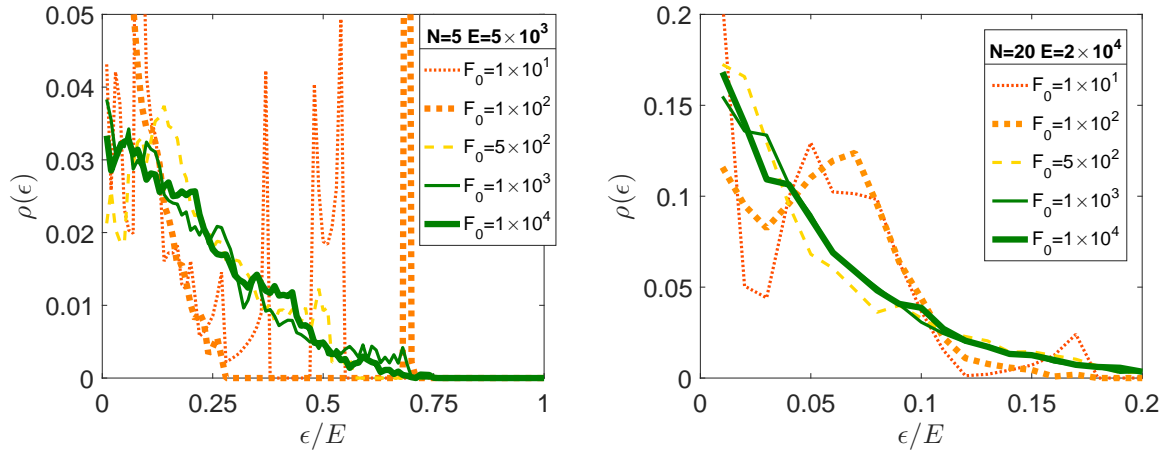
FIG. 9. The distribution of single-particle energies measured in ~ 10000 time units. Green curves obey the relaxation condition (11), and yellow/orange corresponds to smaller F_0. In each panel (different N), we choose E/N identical ($= 1000$), so that the threshold interaction between the two behaviors is $F_0 \sim 1000$.
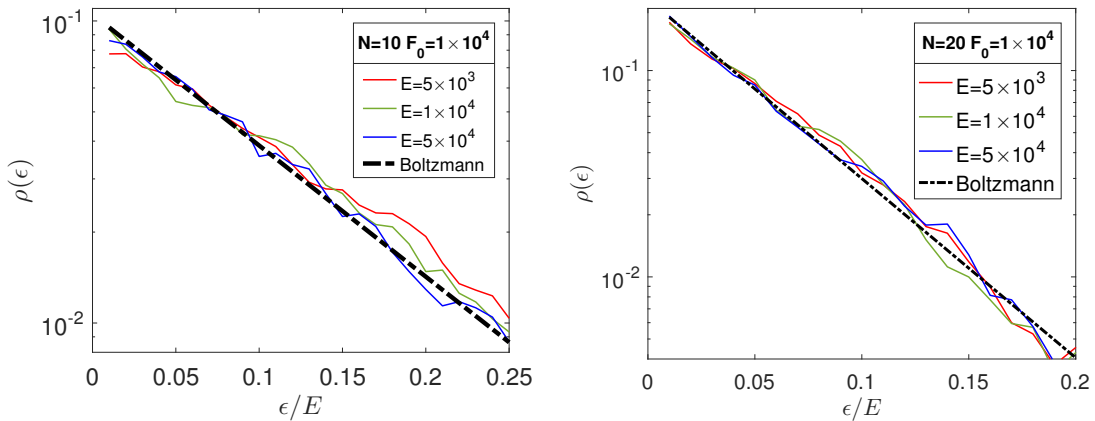

FIG. 10. Comparing the single-particle energy distribution $\rho(\epsilon)$ with the Boltzmann distribution. The energy values all satisfy the relaxation condition (11). The Boltzmann distribution $\propto e^{-\beta \epsilon}$, with the temperature defined as $\beta^{-1} = E/N$, is the thick dashed line.

In Figure 10, we display the agreement with the Boltzmann distribution in several 'thermalizing' situations, $F_0 \gtrsim E/N$. In each panel, the calculated distributions from simulations is plotted against the Boltzmann distribution. The overall agreement shows that the energy is well-thermalized among the particles on average within the timescales under consideration.

There are some small deviations from the Boltzmann distribution visible in Figure 10. Most of the deviation is probably due to numerical noise, and unsurprising given our small system sizes. However, some deviation is also expected due to the contribution of the density of states (DOS). The probability of finding an energy is actually proportional to the Boltzmann exponential factor multiplied by the DOS. For the simple harmonic oscillator, the DOS is constant. The interaction deforms the energy shell in the small region $|x_i - x_j| < \sigma$; so that the DOS is no longer a constant. The measured distribution seems systematically slightly smaller than the Boltzmann curve at very small ϵ: when interaction is weak, particles prefer to stay near zero energy according to the Boltzmann distribution, but when interaction grows, they are no longer allowed to accumulate near zero energy, in other words the DOS at low energy decreases with the increase of interaction. Therefore, counts at the low energy part of Fig.10 is slightly lower than the Boltzmann prediction. The correction to the density of states is not simple to calculate explicitly. Since we are in the regime of a dilute gas ($\sigma \ll R$), the effect is very small.

C.   Lyapunov Exponents

The general idea that thermalization is faster for larger F_0 can be seen through the Lyapunov exponents. For high-dimensional systems, there is a spectrum of exponents which manifests the instability of the trajectory along each direction. The largest Lyapunov exponent (LLE) reflects the shortest time scale for the system lose memory of the initial state. We follow the method described in Ref. [4]. If the calculation is carried out upto sufficiently late times, the LLE for an ergodic system is uniquely defined and independent of the starting state. We would like to deal with parameter regimes both within and outside our relaxation condition $E < F_0 N$ and $E > F_0 N$, and in the latter case we have seen that ergodicity does not become apparent at reasonable timescales. Therefore, we carry out the computation of the LLE upto $t \sim 10^3$, i.e, we consider finite-time Lyapunov exponents (CITE). This means that we can only get initial-configuration-dependent estimates. The collection of these estimates forms a distribution which we show in Figure 11.
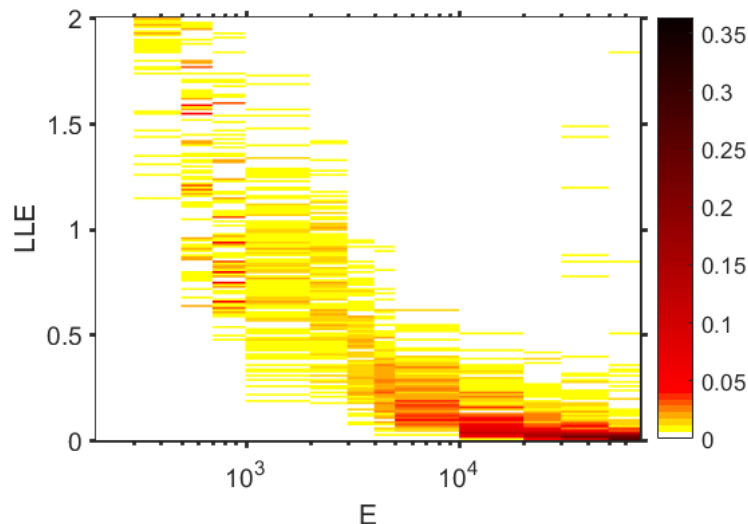

FIG. 11. The distribution of largest Lyapunov exponents, for $N = 5$, $F_0 = 1000$, at different energies. The color indicates the observed probability of a measured LLE value being found in a bin; the bins are of size 0.01.

The LLE decreases with the growth of energy. The critical part is near $E = F_0 N = 5000$. Around this value, the most probable value of LLE decreases well below ~ 1, which indicates that the shortest time scale becomes much longer than an oscillation period when $E \gtrsim 5000$. This is consistent with our predicted thermalization threshold. As E increases far beyond the thermalization threshold value, the LLE distribution is close to zero, suggesting a divergence of relaxation time. We have thus shown an explicit correspondence between energy thermalization in real time and the (finite-time) LLE.

D.   Shape of distribution in single-particle phase space

Till now, we have studied formulated the thermalization question in terms of energy distributions. More generally, thermalization may be taken to mean that a many-body system loses memory of its initial state. In the single-particle phase-space picture, Figures 2 and 3, our initial state is very special: The particles are lined up along the X axis. The effect of interaction is to distort this line toward a circularly symmetric distribution. Thus, we would consider that the memory of the initial state is lost when the distribution of points in the X-P plane are not elongated in any one direction.

To quantify the shape of distribution in phase-space, we define a shape parameter S measuring the degree of ellipticity:

$$S = \frac{a - b}{a + b} \tag{12}$$

where a and b are long axis and short axis of the inertia ellipse in phase space respectively. These are calculated by diagonalizing the inertia tensor I: $I_{xx} = \sum p^2, I_{xp} = I_{px} = -\sum xp, I_{pp} = \sum x^2$. The shape parameter is $S = 1$ for line-shaped distributions and $S = 0$ for circularly symmertic distributions.

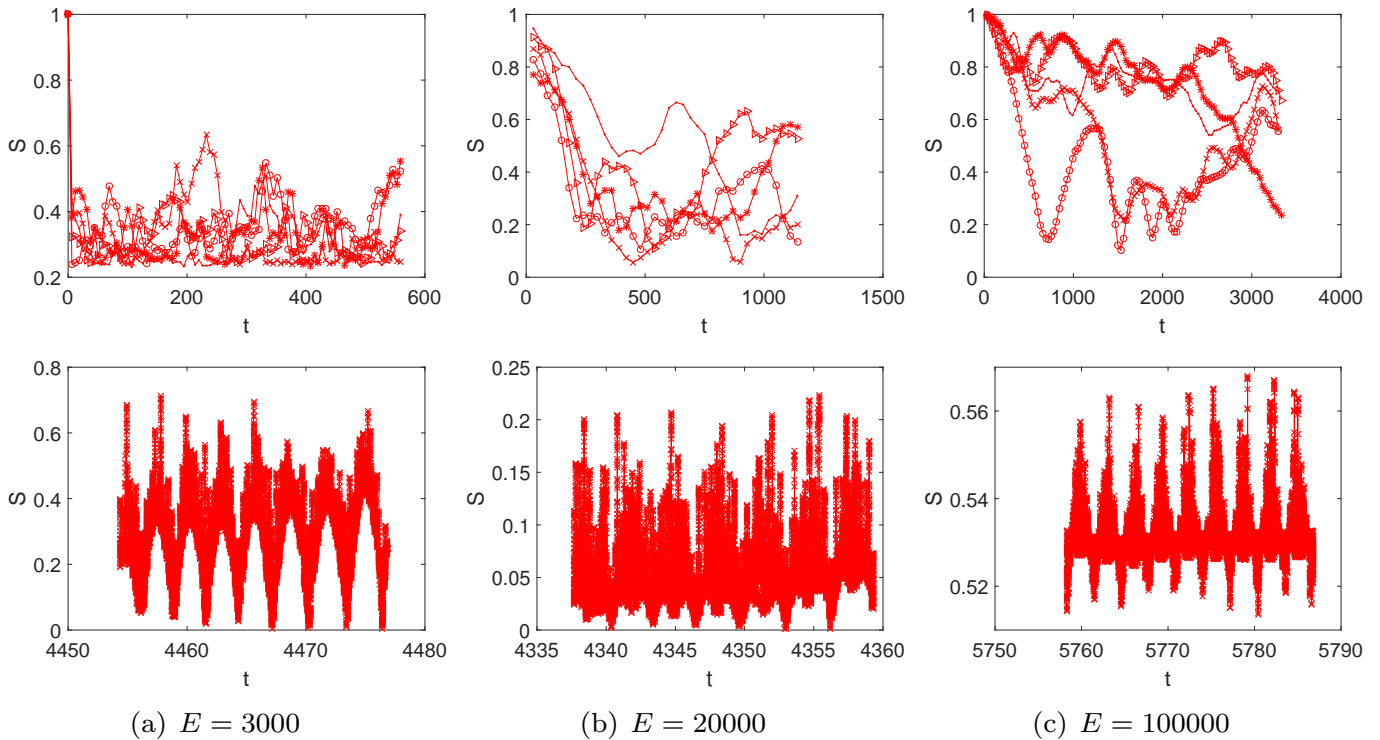(a) $E = 3000$ (b) $E = 20000$ (c) $E = 100000$

FIG. 12. $N = 20, F_0 = 1000$. Time evolution of the shape parameter, $S(t)$, for $N = 20$ particles, $F_0 = 1000$. The three columns correspond to $E < F_0 N$ (low-energy or thermalizing regime), $E = F_0 N$ (intermediate regime), and $E > F_0 N$ (high-energy or non-thermalizing regime). In the top row, coarse-grained values (averaged over 10 periods) are shown, for several initial states with the same energy in each case. The lower row shows original data (not averaged) in a window after several thousand time steps.

The time evolution of the shape parameter S is shown in Fig.12. The top three pannels show averaged values of S in order to highlight the overall behavior. Every data point is the average of the original data over $10T = 20\pi$. The lower six pannels are the original data measured after several thousand time units.

The coarse-grained (averaged) dynamics on top reflects our intuition that there is slower relaxation at larger E/F_0. We see a much faster decay for small E/F_0, i.e., in the thermalizing regime. The behavior of $S(t)$ at longer times shows (lower panel) that there are long-range coherent oscillations of the phase-space cloud shape at rather long timescales. Strikingly, this is even true for the thermalizing regime (lower left panel), for which the time-averaged single-particle energies already are Boltzmann-distributed. Thus, energy thermalization can occur at timescales much faster than it takes for other features of the gas to relax.

V. DISCUSSION AND CONCLUSIONS

Considering classical interacting particles in a harmonic trap, we have addressed two non-equilibrium problems motivated by analogous questions in recent research on quantum many-body dynamics. We have chosen to work with a simple finite-range interaction with variable interaction strength, in the 'dilute gas' regime where the particles are at average distance significantly larger than the interaction range.

The first question concerned the breathing mode of the classical trapped gas, and the influence of interaction on the breathing mode frequency. We have shown nontrivial dependence of the breathing frequency on the interaction strength F_0: the breathing frequency first decreases as a function of F_0, and around the critical value $F_0 \sim E/N$, in increases above the non-interacting value. Eventually at large F_0 the frequency shift reaches a plateau at a value $\propto \sqrt{N^3/E}$. We have explained this behavior physically, using both real-space and phase-space pictures.

The second question concerned the relaxation and thermalization behavior of the gas. This is particularly interesting for a moderate number of particles, far from the thermodynamic limit. We have examined thermalization in the sense of single-particle energy distribution; this has to be carefully defined when the number of particles is in the 'mesoscopic' regime. Sampling the single-particle energies from temporal snapshots of the system over a period of time, we find that

the system 'thermalizes' in reasonable time for $F_0 \gtrsim E/N$. We have explained this condition in terms of relaxation-hindering mechanisms for few-particle systems. We have also shown that this threshold corresponds to the largest finite-time Lyapunov exponent exceeding ≈ 1. Finally, we have found that (for $F_0 > E/N$) thermalization occurs at timescales much faster than the timescale for the breathing mode oscillations to damp out. This is remarkable if one expects thermalization to correspond to the loss of memory of initial conditions: the initial shape ellipticity of the phase space cloud provides very-long-lived oscillations of the shape of the phase space distribution, even after energy thermalization has already occurred.

The present work opens up various questions. Our chosen form of interaction is simple and sensible as a model interaction; and we expect that the F_0-dependence of the breathing mode frequency represents the interaction-dependence for a wide class of interactions. However, it would be interesting to ask how collective modes in general depend on the form of interactions. While the connection between ergodicity and thermalization is expected to be simpler in large systems, for few-body systems like the present case the connection is less clear and raises questions of timescales. Our study of a special case exemplifies the need for better general understanding of the connections between relaxation timescales, interaction strengths, thermalization, and finite-time Lyapunov expnents.

[1] J. P. Dorfman, "An Introduction to Chaos in Non-equilibrium Statistical Mechanics", Cambridge University Press, 1999.
[2] H. S. Dumas: "The KAM Story: A Friendly Introduction to the Content, History, and Significance of Classical Kolmogorov-Arnold-Moser Theory", World Scientific, 2014.
[3] "Boltzmann's Legacy", edited by G. Gallavotti, W. L. Reiter, and J. Yngvason; European Mathematical Society (2007).
[4] J.-P. Eckmann and D. Ruelle, "Ergodic theory of chaos and strange attractors", *Rev. Mod. Phys.*, **57**, 617 (1985).
[5] E. Haller, M. Gustavsson, M. J. Mark, J. G. Danzl, R. Hart, G. Pupillo, H.-C. Nägerl, "Realization of an excited, strongly correlated quantum gas phase," *Science*, **325**, 1224 (2009).
[6] S. Stringari, Phys. Rev. Lett. **77**, 2360 (1996);
M.-O. Mewes, M. R. Andrews, N. J. van Druten, D. M. Kurn, D. S. Durfee, C. G. Townsend, and W. Ketterle, Phys. Rev. Lett. **77**, 988 (1996);
M. Amoruso, I. Meccoli, A. Minguzzi, and M. P. Tosi, Eur. Phys. J. D **8**, 361 (2000);
R. Combescot and X. Leyronas, Phys. Rev. Lett. **89**, 190405 (2002);
F. Chevy, V. Bretin, P. Rosenbusch, K. W. Madison, and J. Dalibard, Phys. Rev. Lett. **88**, 250402 (2002);
C. Menotti and S. Stringari, "Collective oscillations of a one-dimensional trapped Bose-Einstein gas", *Phys. Rev. A* **66**, 043610 (2002).
J. Fuchs, X. Leyronas, and R. Combescot, Phys. Rev. A **68**, 043610 (2003).
[7] L. P. Pitaevskii and A. Rosch, *Phys. Rev. A* **55**, R853 (1997);
[8] H. Moritz, T. Stöferle, M. Köhl, and T. Esslinger, Phys. Rev. Lett. **91**, 250402 (2003).
[9] I. Boettcher, S. Floerchinger, and C. Wetterich, J. Phys. B **44**, 235301 (2011).
[10] W. Tschischik, R. Moessner, M. Haque, Phys. Rev. A **88**, 063636 (2013).
[11] R. Schmitz, S. Krönke, L. Cao, and P. Schmelcher, Phys. Rev. A **88**, 043601 (2013).
[12] I. E. Mazets, "Integrability breakdown in longitudinaly trapped, one-dimensional bosonic gases", *Eur. Phys. J. D* **65**, 43 (2011).
[13] E. Vogt, M. Feld, B. Fröhlich, D. Pertot, M. Koschorreck, and M. Köhl, "Scale Invariance and Viscosity of a Two-Dimensional Fermi Gas", *Phys. Rev. Lett.* **108**, 070404 (2012).
Chao Gao and Zhenhua Yu, "Breathing mode of two-dimensional atomic Fermi gases in harmonic traps", *Phys. Rev. A* **86**, 043609 (2012).
J. Hofmann, "Quantum Anomaly, Universal Relations, and Breathing Mode of a Two-Dimensional Fermi Gas", *Phys. Rev. Lett.* **108**, 185303 (2012).
S. K. Baur, E. Vogt, M. Köhl, and G. M. Bruun, "Collective modes of a two-dimensional spin-1/2 Fermi gas in a harmonic trap", *Phys. Rev. A* **87**, 043612 (2013).
B. P. van Zyl, E. Zaremba, and J. Towers, "Collective excitations of a harmonically trapped, two-dimensional, spin-polarized dipolar Fermi gas in the hydrodynamic regime", *Phys. Rev. A* **90**, 043621 (2014).
Yi-Cai Zhang and Shizhong Zhang, "Strongly interacting p -wave Fermi gas in two dimensions: Universal relations and breathing mode", *Phys. Rev. A* **95**, 023603 (2017).
[14] G. De Rosi and S. Stringari, "Collective oscillations of a trapped quantum gas in low dimensions", *Phys. Rev. A* **92**, 053617 (2015).
[15] S. Riedl, E. R. Sánchez Guajardo, C. Kohstall, A. Altmeyer, M. J. Wright, J. Hecker Denschlag, R. Grimm, G. M. Bruun, and H. Smith, "Collective oscillations of a Fermi gas in the unitarity limit: Temperature effects and the role of pair correlations", Phys. Rev. A **78**, 053609 (2008).
[16] B. Fang, G. Carleo, A. Johnson, and I. Bouchoule, Phys. Rev. Lett. **113**, 035301 (2014).
[17] W. Tschischik and M. Haque, Phys. Rev. A **91**, 053607 (2015).
[18] W. Tschischik, R. Moessner, and M. Haque, "Bose-Hubbard ladder subject to effective magnetic field: Quench dynamics in a harmonic trap", *Phys. Rev. A*, **92**, 023845 (2015).

[19] M. Cominotti, F. Hekking, and A. Minguzzi, arXiv:1503.07776.

[20] S. Chen, L. Guan, X. Yin, Y. Hao, and X-W. Guan, Phys. Rev. A **81**, 031609(R) (2010).

[21] G. E. Astrakharchik, J. Boronat, J. Casulleras, and S. Giorgini, Phys. Rev. Lett. **95**, 190407 (2005).

[22] A. Iu. Gudyma, G. E. Astrakharchik, and M. B. Zvonarev, "Reentrant behavior of the breathing-mode-oscillation frequency in a one-dimensional Bose gas", Phys. Rev. A **92**, 021601(R) (2015).
S. Choi, V. Dunjko, Z. D. Zhang, and M. Olshanii, "Monopole Excitations of a Harmonically Trapped One-Dimensional Bose Gas from the Ideal Gas to the Tonks-Girardeau Regime", *Phys. Rev. Lett.* **115**, 115302 (2015)
X.-L. Chen, Y. Li, and H. Hu, Phys. Rev. A **91**, 063631 (2015).

[23] S. Bauch, K. Balzer, C. Henning, and M. Bonitz, Phys. Rev. B **80**, 054515 (2009);
J. W. Abraham, K. Balzer, D. Hochstuhl, and M. Bonitz, Phys. Rev. B **86**, 125112 (2012);
C. R. McDonald, G. Orlando, J. W. Abraham, D. Hochstuhl, M. Bonitz, and T. Brabec, Phys. Rev. Lett. **111**, 256801 (2013);
J. W. Abraham, M. Bonitz, C. McDonald, G. Orlando, and T. Brabec, New J. Phys **16**, 013001 (2014).

[24] J. W. Abraham, and M. Bonitz, "Quantum Breathing Mode of Trapped Particles: from nanoplasmas to ultracold gases", *Contributions to Plasma Physics*, **54**, 27 (2014).

[25] L. Brey, N. F. Johnson, and B. I. Halperin, Phys. Rev. B **40**, 10647 (1989).
M. Bonitz, K. Balzer, and R. van Leeuwen, *Phys. Rev. B* **76**, 045341 (2007).

[26] T. Kinoshita, T. Wenger, and D. S. Weiss, "A quantum Newton's cradle", *Nature*, **440,** 900 (2006).

[27] B. Doyon and H. Spohn, "Dynamics of hard rods with initial domain wall state", *J. Stat. Mech.*, **2017**, 073210 (2017).

[28] X. Cao, V. B. Bulchandani, J. E. Moore, "Incomplete thermalization from trap-induced integrability breaking: lessons from classical hard rods", arXiv:1710.09330.

[29] D. Guéry-Odelin, F. Zambelli, J. Dalibard, and S. Stringari, "Collective oscillations of a classical gas confined in harmonic traps," *Phys. Rev. A*, **60**, 4851 (1999).

[30] D. S. Lobser, A. E. S. Barentine, E. A. Cornell, and H. J. Lewandowski, "Observation of a persistent non-equilibrium state in cold atoms", Nat Phys **11**, 1009 (2015).

[31] F. Dalfovo, S. Giorgini, M. Guilleumas, L. Pitaevskii, and S. Stringari, "Collective and single-particle excitations of a trapped bose gas," *Phys. Rev. A*, **56**, 3840 (1997).

[32] D. S. Jin, J. R. Ensher, M. R. Matthews, C. E. Wieman, and E. A. Cornell, "Collective excitations of a bose-einstein condensate in a dilute gas," *Phys. Rev. Lett.*, vol. 77, pp. 420–423, July 1996.

[33] F. Dalfovo, S. Giorgini, L. P. Pitaevskii, and S. Stringari, "Theory of bose-einstein condensation in trapped gases," *Rev. Mod. Phys.*, vol. 71, pp. 463–512, Apr. 1999.

[34] S. Stringari, "Collective excitations of a trapped bose-condensed gas," *Phys. Rev. Lett.*, vol. 77, pp. 2360–2363, Sept. 1996.

[35] T. Tsuchiya and N. Gouda, "Relaxation and Lyapunov time scales in a one-dimensional gravitating sheet system," *Phys. Rev. E*, **61**, 948 (2000).

[36] K. R. Yawn and B. N. Miller, "Ergodic properties and equilibrium of one-dimensional self-gravitating systems," *Phys. Rev. E*, vol. 56, pp. 2429–2436, Sept. 1997.

[37] F. Jin, T. Neuhaus, K. Michielsen, S. Miyashita, M. A. Novotny, M. I. Katsnelson, and H. D. Raedt, "Equilibration and thermalization of classical systems," *New Journal of Physics*, vol. 15, no. 3, p. 033009, 2013.

[38] M. Anderlini and D. Guéry-Odelin, "Thermalization in mixtures of ultracold gases", *Phys. Rev. A* **73**, 032706 (2006).